ON THE MAGNETIC STRUCTURE OF THE QUIET TRANSITION REGION

JAMES F. DOWDY, JR.

Graduate Co-op at the University of Alabama in Huntsville assigned to Space Science Laboratory, NASA Marshall Space Flight Center, Code ES52, Huntsville, AL 35812, U.S.A.

DOUGLAS RABIN

National Solar Observatory, National Optical Astronomy Observatories, Tucson, AZ 85726, U.S.A.*

and

RONALD L. MOORE

Space Science Laboratory, NASA Marshall Space Flight Center, Code ES52, Huntsville, AL 35812, U.S.A.

(Received 17 January, 1986)

Abstract. Existing models of the quiet chromosphere–corona transition region predict a distribution of emission measure over temperature that agrees with observation for $T \gtrsim 10^5$ K. These 'network' models assume that all magnetic field lines that emerge from the photosphere extend into and are in thermal contact with the corona. We show that the observed fine-scale structure of the photospheric magnetic network instead suggests a two-component picture in which magnetic funnels that open into the corona emerge from only a fraction of the network. The gas that makes up the hotter transition region is mostly contained within these funnels, as in standard models, but, because the funnels are more constricted in our picture, the heat flowing into the cooler transition region from the corona is reduced by up to an order of magnitude. The remainder of the network is occupied by a population of low-lying loops with lengths $\lesssim 10^4$ km. We propose that the cooler transition region is mainly located within such loops, which are magnetically insulated from the corona and must, therefore, be heated internally. The fine-scale structure of ultraviolet spectroheliograms is consistent with this proposal, and theoretical models of internally heated loops can explain the behavior of the emission measure below $T \approx 10^5$ K.

1. Introduction

The structure of the chromosphere–corona transition region is dictated by the structure of its magnetic field: because the magnetic pressure dominates the gas pressure, mass and energy flows are channeled by field lines. We can expect to improve our understanding of the transition region by improving our picture of its magnetic field.

Figure 1 illustrates the standard magnetic picture of the quiet transition region (Gabriel, 1976; Athay, 1981a): magnetic field lines emerge from the boundaries of supergranules and fan out rapidly with height to fill the corona. From the viewpoint of the corona, all field lines are funneled into the network. The transition region is just the necessary thermal connection between the hot corona and the cool chromosphere, and all the energy needed to maintain the transition layer is supplied by a flow of heat from the corona ('back heating'). Gabriel (1976) showed that the thin transition layer occurs

* Operated by the Association of Universities for Research in Astronomy, Inc., under contract with the National Science Foundation.

Solar Physics **105** (1986) 35–45.

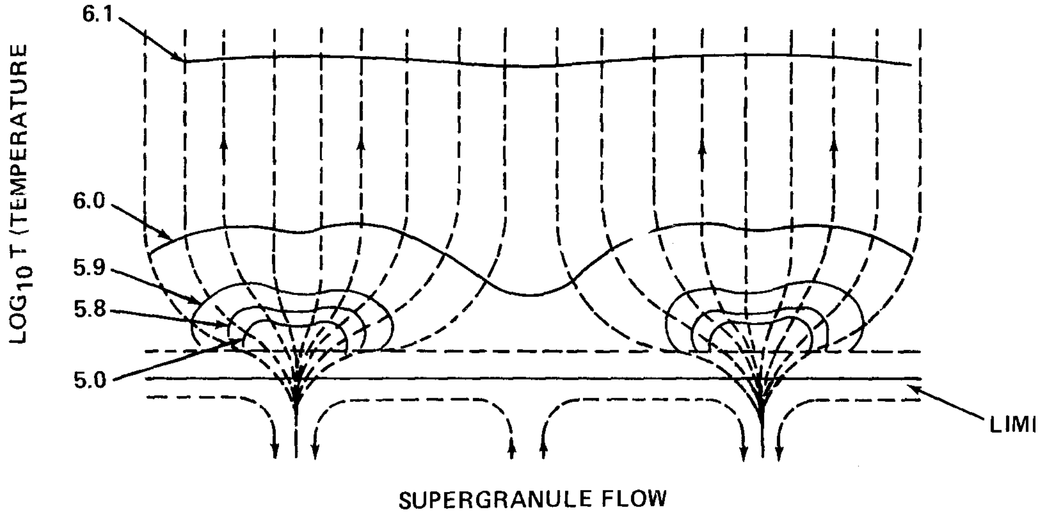

Fig. 1. The standard two-dimensional picture of magnetic structure in the transition region (after Gabriel, 1976). Field lines emerge from the network boundaries, where they are concentrated by supergranulation flow and from where they diverge rapidly with height until they are uniform and vertical in the corona. All of the flux that emerges from the surface eventually reaches the corona. It is tacitly assumed that the magnetic field is approximately uniform along the cell boundaries.

in the throats of the coronal funnels, so the standard model is consistent with the observation that ultraviolet emission from the transition region is largely confined to the network defined by the photospheric magnetic field. The standard model is also successful in reproducing the run of emission measure with temperature in the hotter part of the transition region, $T \gtrsim 10^5$ K. However, back-heating models have so far failed to reproduce even approximately the behavior of the emission measure in the cooler transition region, $T \lesssim 10^5$ K (Athay, 1981a, 1982)*.

In the process of meeting one observational requirement – that coronal field lines originate in the magnetic network – the standard model tacitly includes another assumption that is not obviously required by observation: that all field lines that originate in the network reach, and are in thermal contact with, the corona. In this paper we argue that the observed fine-scale structure of the photospheric magnetic field and the observed fine-scale structure of the transition region together suggest a picture of the magnetic transition region that differs essentially from the standard picture. In our view, although some of the magnetic field is in funnels that open into the corona as in Figure 1, the rest of the field is in small loops that close within the network. We identify this dichotomy with the observed dichotomy of the transition region as reflected in its emission measure. The hotter transition region resides mainly in the open funnels and is maintained by back heating, as in the standard model. However, little of the cooler transition region is in the throats of the funnels; it is mostly contained within the small

* We use the terms 'hotter' and 'cooler' in preference to the conventional terms 'upper' and 'lower' because the implication of vertical stratification is incorrect in our magnetic picture.

loops. The magnetic field along these loops strongly inhibits the flow of heat and gas across them, so the gas within is effectively insulated from the corona and the hotter transition region. Therefore, the cooler transition region must be heated internally rather than by back heating.

The notion that the cooler transition region is structurally distinct from the hotter transition region has been proposed previously by Feldman (1983) and by Rabin and Moore (1984) on the basis of observed spatial structure, mass motions, and emission measure in the transition region. In this paper, we show how this view is supported by the structure of the magnetic field observed in the photosphere, and we point out that a revised picture of the magnetic transition region bears on the energetics of the corona as well.

2. Magnetic Structure of the Network

Figure 2 shows extreme ultraviolet spectroheliograms of a quiet region acquired by the Harvard instrument on *Skylab* (Reeves *et al.*, 1976). A network pattern is evident over

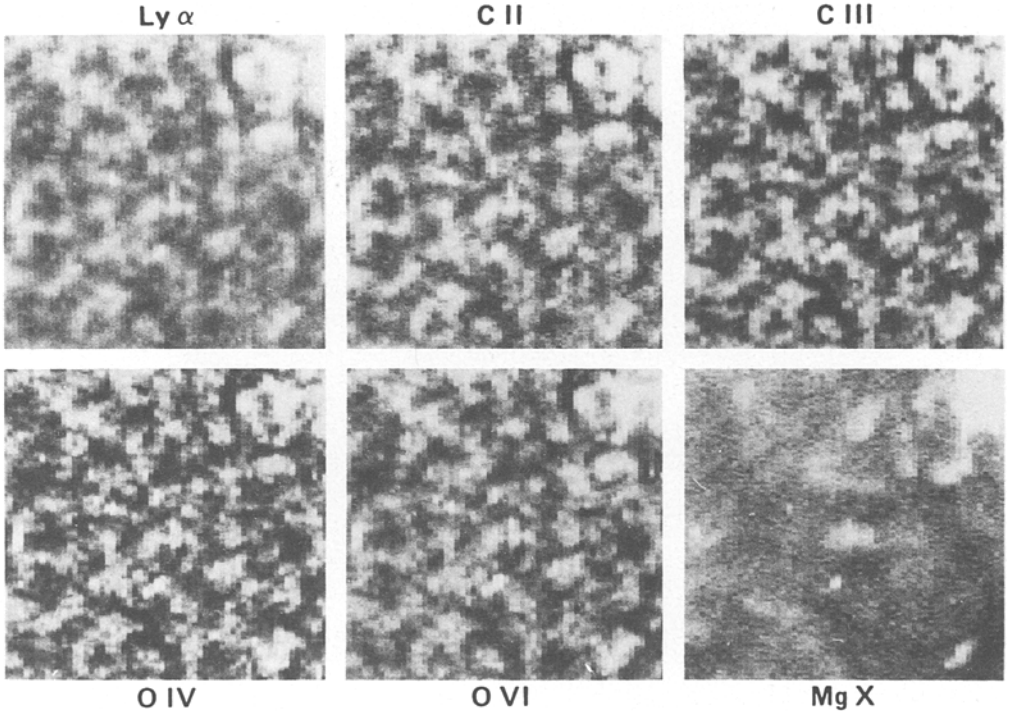

Fig. 2. Spectroheliograms of the quiet network in emission lines of Lα and C II (2×10^4 K), C III (7×10^4 K), O IV (1.5×10^5 K), and O VI (3×10^5 K) in the transition region, and Mg X (1.4×10^6 K) in the corona, taken with the Harvard spectrometer on *Skylab* and reported by Reeves *et al.* (1976). In transition region emission, the network lanes are seen to outline nearly complete cells, but the lanes themselves are very nonuniform. Large fluctuations of intensity from pixel to pixel (5″ resolution) within the network lanes are evident. The network is much less noticeable in the corona. The field of view is 5′ square, positioned midway to the limb; each pixel is 5″ square.

the temperature range bounded by Lα and O VI ($2 \times 10^4 \lesssim T \lesssim 3 \times 10^5$), but the emission is clumpy and irregular along the network. In Figure 3, a photospheric

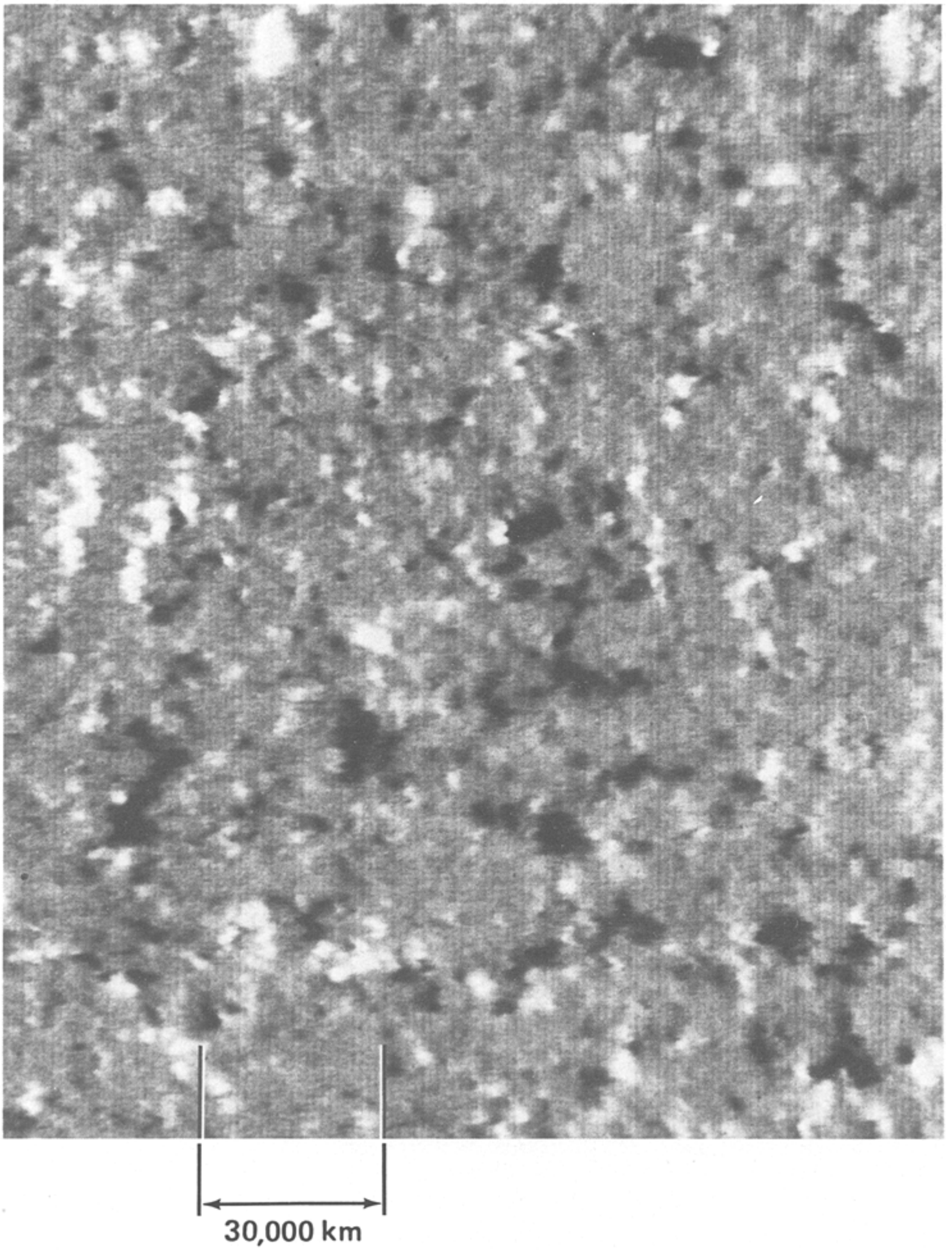

Fig. 3. High-resolution magnetogram of the quiet Sun at disk center taken at Kitt Peak (resolution $\approx 2''$). The magnetic flux is concentrated in a loose network, the same network seen in the chromosphere and transition region. The magnetic flux within the network lanes is very irregular, and polarities are a 'salt and pepper' mix of positive and negative, predominantly on spatial scales much less than a supergranule diameter: the diameters of unipolar patches of flux and the separations between neighboring patches of opposite polarity range from $\approx 10''$ down to the limit of resolution.

magnetogram of another quiet area (Livingston and Harvey, 1975) conveys a similar impression of clumpiness along the network. This would seem to suggest that the standard model of the transition region need only be slightly modified, to incorporate three-dimensional rather than strictly two-dimensional magnetic funneling, in order to be consistent with the ultraviolet and magnetic observations. However, this overlooks another striking feature of the magnetogram in Figure 3: the intimate mixture of magnetic polarities along the network. In nearly every 10^4 km segment of the network, there is some flux of both polarities. The intermixing of polarities is a general trait of quiet regions; in magnetograms with the spatial resolution and sensitivity of the one in Figure 3, a mixture of polarities is always seen on supergranular scales (Giovanelli, 1982).

If the magnetogram in Figure 3 were used as a boundary condition to calculate the potential magnetic field above the photosphere, the resulting field would contain many small-scale magnetic loops with lengths and heights less than 10^4 km, corresponding to the separation of clumps of opposite polarity*. Of course the polarities are not exactly balanced, so some field lines must extend higher into the atmosphere, either to return at some distant site or to continue into the solar wind. Thus, the photospheric magnetogram suggests a two-component structure to the magnetic field over the network: an open component that emerges from distinct clumps along the network and fans out in three dimensions to cover the interiors of the supergranules; and a closed component consisting of smaller loops (length $\lesssim 10^4$ km) that emerge and return within the network lane.

The open component is similar to the coronal funnels of the standard model, and we expect the thermal structure of the transition region in the open component to closely resemble the standard model. Figure 4 illustrates the typical observed run of emission measure for a quiet area together with the prediction of a refined network model that incorporates a realistic large-scale magnetic geometry and steady gas flow (Athay, 1982). The model agrees fairly well with the observations for $T \gtrsim 10^5$ K, so there is no reason to alter the conventional view that the hotter transition region is mainly contained in the throats of coronal funnels. However, because the marked failure below $T \approx 10^5$ K does not appear to be remediable within the context of the standard model (Athay, 1982), we shall assume that the bulk of the gas that constitutes the cooler transition region is not in the coronal funnels. Our hypothesis is that it is contained in the second magnetic component of the network, the low-lying loops.

There is some direct evidence that the cooler transition region is in small loops. Filtergrams in Lα ($T \approx 2 \times 10^4$ K) with spatial resolution of 1″ (Bonnet *et al.*, 1980) plainly show loops in and around active regions. The structure of the Lα network is less clear, but Bonnet *et al.* (1980) report from inspection of the original photographs that 'the chromospheric network seems to consist of individual bright loops'.

* Even if the field is non-potential, there should be small-scale loops. The only way to avoid this would be to envision closely packed funnels with oppositely directed magnetic fields, implying that the corona above a quiet region is riddled with large-scale current sheets. On the contrary, on scales larger than $\approx 10^4$ km, observed coronal loops show that the field is potential to first order (Sheeley, 1981).

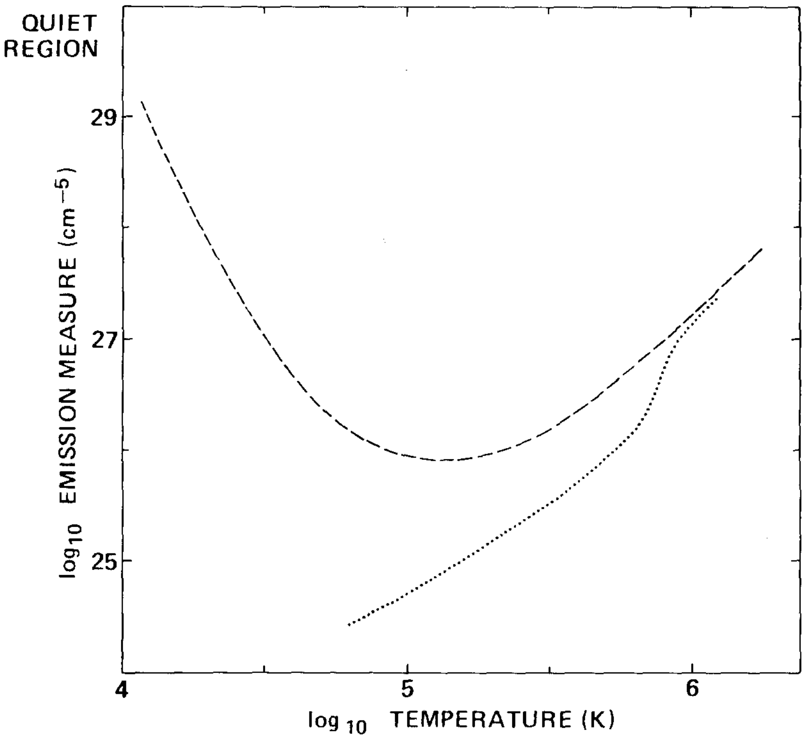

Fig. 4. Distribution of emission measure with temperature through the quiet transition region (after Rabin and Moore, 1984). The dashed line is derived from observation. The dotted line is derived from an energy balance model (Athay, 1982) which incorporated standard magnetic field structure (see Figure 1) and balanced radiative losses with downward thermal conduction and enthalpy flux from the corona. Such models account for the hotter branch of the observed emission measure curve, but not the cooler branch.

Because magnetic polarities are intermixed within the width of the network (on scales $\lesssim 10^4$ km), most of the network loops will be of that length (and height) or less. This is compatible with the observed extension of the cooler transition region above the limb. Emission from the cooler transition region falls off with a scale height of about 2000 km but persists to heights of about 10^4 km over the full range of temperature (Feldman *et al.*, 1979; Withbroe, 1983). The intermixing of the loops with the throats of the coronal funnels is compatible with the observed peak emission from the hotter transition region being well below 10^4 km, that is, well within the height range of the cooler transition region (Huber *et al.*, 1974; Withbroe, 1983).

We would expect that the two magnetic components – network loops and coronal funnels – would intermingle on the same scales that magnetic polarities intermingle. Figure 3 shows mixed polarities on every scale down to the limit of resolution (about 2″), and indeed the finest scales have the most pronounced 'salt and pepper' appearance. There is no reason to suppose that the finest extent of intermixing has yet been resolved. Therefore, within the context of the proposed model, network loops and coronal funnels should intermingle on spatial scales less than about 10″ everywhere within the network, and in many places on scales as small as 1″ or less. This is consistent with the appearance of the *EUV* spectroheliograms in Figure 2, which have 5″ pixels. Emission from the cooler part of the hotter transition region (O VI) originates in the throats of coronal funnels, where they are not greatly wider than their photospheric roots. Cooler lines (C II, C III) are formed in the network loops. Yet, the structure of the O VI image closely matches the structure of the cooler transition region images. This is compatible with the intermixing of coronal funnels and network loops on scales less than 10″.

More extreme structural coincidence is expected for the standard model, in which the hotter and cooler transition regions are both in the open component. Because of the thinness of the transition region in the standard model, no appreciable difference between hotter and cooler transition region images should appear until the resolution reaches subarcsecond scales. Close comparison of the hotter transition region image (O VI) in Figure 2 with the cooler transition region images and comparison of brightness traces along network lanes (Reeves, 1976) show definite differences at several small sites, each only 1 or 2 pixels in area. The differences cannot be explained with the standard picture. Can our revised picture account for them? In the magnetogram of Figure 3, there are some unipolar patches 5–10″ across. For our picture, we would expect the interiors of these patches to be mostly occupied by the feet of coronal funnels and, hence, cooler transition region emission would be deficient in the middle of these patches even with pixels as large as those in Figure 2 (5″). Judging from the magnetogram in Figure 3, we expect many more places of difference to become visible as the resolution is improved below 5″. In observations of the cooler transition region with much better resolution than in Figure 2 (Bonnet *et al.*, 1980; Dere *et al.*, 1984), the network lanes are full of fine structure at 1–2″. However, there are yet no images of the hotter transition region with resolution better than in Figure 2, so our expectation of increasing spatial differentiation between the hotter and cooler transition region with increasing resolution below 5″ remains a prediction.

3. Discussion

Figure 5 summarizes in cartoon form our picture of the magnetic transition region. The network is a 'magnetic junkyard' whose main features are:

(1) A new magnetic component, the network loops. These loops contain most of the cooler transition region, $T \lesssim 10^5$ K. Because the loops are magnetically insulated from the corona, the gas within them cannot be heated by energy transferred from the corona. The bulk of the cooler transition region must be internally heated.

(2) Coronal funnels, which contain most of the hotter transition region. The hotter transition region is sustained by back heating, as in the standard model. Although some cooler transition region gas is also located in the feet of the funnels, it contributes negligibly to the emission measure below 10^5 K. Emerging from only a fraction of the network lane, the funnels are more constricted than the magnetic channels of the standard model.

It is of interest to estimate the constriction factor of the coronal funnels through the

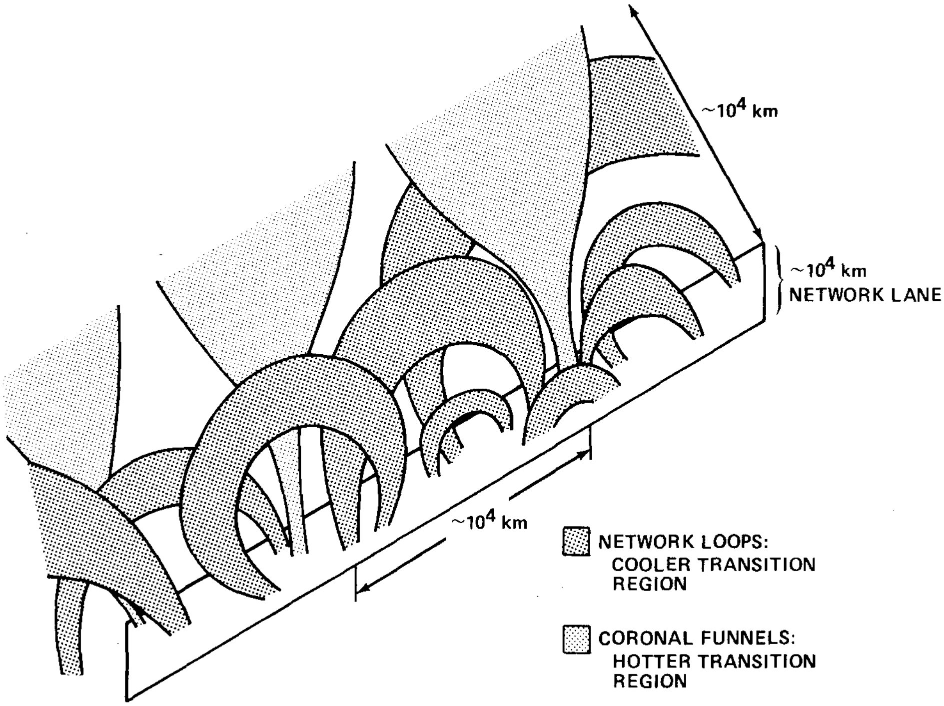

Fig. 5. Our three-dimensional picture for the magnetic structure of the quiet transition region. A 'magnetic junkyard' is collected into the network lanes by supergranulation flow. There are two distinct populations of magnetic structures: (1) network loops, low-lying loops within the network lanes, and (2) coronal funnels, comprised of open field lines reaching up into the corona. We expect that most of the cooler transition region is in the network loops. The coronal funnels resemble the structures in the standard picture (Figure 1) and contain a similar conductive transition region, but they are more constricted in this picture due to crowding by the network loops. Thus, although some cooler transition region plasma is contained in the funnels, the area in the lower part of the flux tube is reduced too much to make a major contribution to the emission. On the other hand, the field lines diverge rapidly enough to account for the entire hotter transition region in a manner similar to the standard picture. The cooler transition region plasma in the network loops is magnetically insulated from the corona and so must be heated internally rather than by heat transfer from the corona.

hotter transition region. In models based on the standard picture, this factor is just the inverse of the fraction of surface area occupied by the cooler transition region. At 5″ resolution, the network appears to occupy nearly half of the surface, as in Figure 2. At the best resolution achieved to date, about 1″, the network viewed in C IV emission appears to occupy about 15% of the surface (Dere *et al.*, 1984). Gabriel's (1976) network model has a constriction factor of about 3; Athay (1981a, 1982) has taken a constriction factor of 10. However, measurements of the photospheric magnetic field indicate that the constriction factor in our picture is typically much greater than 10.

The coronal magnetic field is given by the net photospheric field over supergranular areas. From magnetograms obtained with a 1.3×10^4 km aperture, Howard and LaBonte (1981) found the average field strength in quiet regions to be about 2 G. We expect coronal funnels to be mostly rooted in the larger patches of flux in the network, such as those seen in Figure 3. The apparent photospheric field strength in such patches is typically several hundred gauss (Harvey, 1976). Thus, 100 G is probably a low estimate of field strengths for cooler transition region plasma in the feet of funnels, no more than a few thousand kilometers above the photosphere. We therefore estimate that the typical constriction factor for field lines which pass through the hotter transition region is of order 100.

Dowdy *et al.* (1985) have examined the reduction of conductive heat flow by magnetic constriction in the transition region. They show that, for three-dimensional constriction as in the funnels in our network picture, the heat flow reduction factor is approximately the square root of the constriction factor. Hence, the reduction factor for heat flow through the hotter transition region is ≈ 10. Thus, the constriction alone should substantially reduce the possible heat flow from the corona to the cooler transition region from that in the standard picture. This only aggravates the failure of back heating to sustain the cooler transition region.

If back heating supplied the radiative loss from the cooler transition region in addition to that from the hotter transition region, then this would be the dominant energy loss from the corona. In quiet regions, the radiative loss from the cooler transition, including Lα, is about 3×10^5 erg cm^{-2} s^{-1}, the radiative loss from the hotter transition region is about 1×10^5 erg cm^{-2} s^{-1}, and the radiative plus solar wind energy loss rate from the corona is about 1×10^5 erg cm^{-2} s^{-1} (Athay, 1981b; Withbroe and Noyes, 1977). Thus, if the cooler transition region is heated internally rather than by back heating, the total heating requirement for the quiet corona is reduced from about 5×10^5 erg cm^{-2} s^{-1} to about 2×10^5 erg cm^{-2} s^{-1}, and the energy loss from the corona to the transition region amounts to only about half of the total heating required to sustain the corona.

Can placing the cooler transition region in network loops address the basic problem of explaining the observed rise in emission measure below 10^5 K (Figure 4)? Two recent models suggest that it can.

Rabin and Moore (1984) postulate a specific heating mechanism: classical ohmic dissipation of field-aligned electric currents. The required current elements are sufficiently thin ($\lesssim 1$ km) that their heat escapes mainly by conduction across the magnetic field, and the slope of the emission measure below 10^5 K is a natural consequence of the temperature dependence of cross-field thermal conduction. The central question in this model is the origin of the extremely filamentary nature of the currents that it requires.

In the model of Antiochos and Noci (1985), the heating mechanism is unspecified. They point out that for magnetic loops the static energy-balance equations admit a cool ($T \lesssim 10^5$ K), nearly isothermal solution as well as the usual coronal solution. For low-lying loops ($h \lesssim 5000$ km), the isothermal solution is stable, but the coronal solution is unstable. This indicates that low-lying loops should be nearly isothermal. The differential emission measure produced by a single loop is too shallow to account for Figure 4. In this model, agreement with observation must be secured by supposing that the distribution of cool loops of different temperature is such that their superposed emission measure has the required slope.

Even though these two models are preliminary in character, it is encouraging that ideas based on internal heating of the cooler transition region have more success than models that rely on energy transfer from the corona.

We have not thus far considered the dynamics of the transition region. In the cooler transition region, there are two main aspects. First, averaged over large areas, a mean downflow of about 10 km s^{-1} is observed at $T \approx 10^5$ K (Doschek *et al.*, 1976). Second, the visual appearance of the cooler transition region above the limb is spiky, reminiscent of Hα spicules, and the scale height of this emission is comparable to that of spicules (Withbroe, 1983). This suggests that the fine-scale dynamics of the cooler transition region may resemble the dynamics of spicules, and, indeed, Dere *et al.* (1983) have observed instances of transient upflows in the cooler transition region on the spatial scale of spicules.

In the context of our model, these observations imply that the cooler transition region within the network loops must be dynamic. Dynamic models of internally heated cooler transition region loops have not yet been constructed. Some heating mechanisms, such as the electric currents proposed by Rabin and Moore (1984), operate on short enough time-scales that they might apply to dynamic loops without basic change in character.

Once it is admitted that the heating of the transition region may be a fundamentally time-dependent process involving internal heating and cooling in spicule-like events, it may be possible to produce both the hotter and the cooler transition regions in the same magnetic structure, such as the coronal funnels. Athay (1984) has considered a model of this kind. Comparison of cooler transition region structures to Hα spicules may help to discriminate between the network loop picture and models such as Athay's. It will be of interest to investigate observationally whether spicules occur primarily in open-field or closed-field configurations.

Since our picture has been presented with reference to the magnetogram in Figure 3, we should ask how representative that magnetogram is of quiet region fields in general. This question was investigated by Giovanelli (1982). He found that the mixture of opposite polarities is sometimes nearly complete, so that there is very little net flux over the scale of a supergranule and larger. However, even in so-called 'unipolar' quiet regions, at least 10% (by flux) of the polarity opposite to the dominant polarity is always present in magnetograms of the quality of Figure 3. Thus, a loop component of the network should always be present, but the fraction of the network that it occupies and its importance relative to the coronal funnels should vary considerably between quiet regions. This raises the question, whether the ratio of cooler to hotter transition region emission also varies with the degree of unipolarity of the network. Our model suggests that it should.

The recognition that much of the magnetic network consists of small loops that may contain most of the cooler transition region focuses attention on the need for internal heating of the cooler transition region. This is the central point of this paper.

Acknowledgements

We are grateful to G. Withbroe for supplying the *EUV* spectroheliograms in Figure 2 and to J. W. Harvey for the magnetogram in Figure 3. We thank J. Porter and M. Machado for suggestions which improved the presentation. This work was supported by funding from the NASA Office of Solar and Heliospheric Physics for research at MSFC on solar magnetic fields. In addition, J. Dowdy received support from NASA contract NAGW-294 and NSF contract ATM-8505475.

References

Antiochos, S. K. and Noci, G.: 1985, 'The Structure of the Static Corona and Transition Region', Preprint No. CSSA-ASTRO-85-13.

Athay, R. G.: 1981a, *Astrophys. J.* **249**, 340.

Athay, R. G.: 1981b, in S. Jordan (ed.), *The Sun as a Star*, NASA SP-450, p. 85.

Athay, R. G.: 1982, *Astrophys. J.* **263**, 982.

Bonnet, R. M., Bruner, E. C., Jr., Acton, L. W., Brown, W. A., and Decaudin, M.: 1980, *Astrophys. J.* **237**, L47.

Dere, K. P., Bartoe, J.-D. F., and Brueckner, G. E.: 1983, *Astrophys. J.* **267**, L65.

Dere, K. P., Bartoe, J.-D. F., and Brueckner, G. E.: 1984, *Astrophys. J.* **281**, 870.

Doschek, G. A., Feldman, U., and Bohlin, J. D.: 1976, *Astrophys. J.* **205**, L177.

Dowdy, J. F., Moore, R. L., and Wu, S. T.: 1985, *Solar Phys.* **99**, 79.

Feldman, U.: 1983, *Astrophys. J.* **275**, 367.

Feldman, U., Doschek, G. A., and Mariska, J. T.: 1979, *Astrophys. J.* **229**, 369.

Gabriel, A. H.: 1976, *Phil. Trans. Roy. Soc. London* **A281**, 339.

Giovanelli, R. G.: 1982, *Solar Phys.* **77**, 27.

Harvey, J.: 1976, in E. A. Muller (ed.), *IAU Highlights of Astronomy*, Vol. 4, Part II.

Howard, R. and LaBonte, B. J.: 1981, *Solar Phys.* **74**, 131.

Huber, M. C. E., Foukal, P. V., Noyes, R. W., Reeves, E. M., Schmahl, E. J., Timothy, J. G., Vernazza, J. E., and Withbroe, G. L.: 1974, *Astrophys. J.* **194**, L115.

Livingston, W. C. and Harvey, J.: 1975, *Bull. Am. Astron. Soc.* **7**, 346.

Rabin, D. and Moore, R.: 1984, *Astrophys. J.* **285**, 359.

Reeves, E. M.: 1976, *Solar Phys.* **46**, 53.

Reeves, E. M., Vernazza, J. E., and Withbroe, G. L.: 1976, *Phil. Trans. Roy. Soc. London* **A281**, 319.

Sheeley, N. R., Jr.: 1981, in F. Q. Orrall (ed.), *Solar Active Regions*, Colorado Associated University Press, Boulder, p. 17.

Withbroe, G. L.: 1983, *Astrophys. J.* **267**, 825.

Withbroe, G. L. and Noyes, R. W.: 1977, *Ann. Rev. Astron. Astrophys.* **15**, 363.